Publication Date: 30 June 2026
Archs Sci. (2026) Volume 75, Issue 3 Pages 34-45, Paper ID 2025304.

Integrating Micro-Morphological Identification and Biomechanical Analysis for the Quality Assessment of Traditional Chinese Medicinal Materials

Yaling Gao
Department of Pharmaceutical Engineering, Hebei Chemical & Pharmaceutical College, Shijiazhuang 050026, Hebei Province, China
Corresponding author: Yaling Gao Email: zhiyaoxi319361@163.com

Abstract The authentication and quality evaluation of traditional Chinese medicinal (TCM) materials remain critical challenges because of the widespread presence of counterfeit and adulterated products in modern markets. Although traditional sensory identification methods remain widely employed in professional practice, these methods are affected by subjectivity, limited observational resolution, and susceptibility to deliberate deception. In response to these limitations, this study presents a comprehensive analytical framework that integrates micro-morphological identification with biomechanical interpretation to improve the accuracy, reliability, and scientific validity of TCM material authentication and quality assessment. Using high-resolution stereomicroscopy, ultraviolet fluorescence imaging, and extended-depth-of-field (EDF) image synthesis, we analyzed the microstructures of several commonly used TCM materials, including *Aurantii Fructus*, *Amomum villosum*, *Atractylodis Rhizoma*, and *Ziziphi Spinosae Semen*. The analyses were conducted to identify and characterize important anatomical markers, including oil-chamber density, surface-spine morphology, fiber width, glandular distribution, and cell-wall thickness. These distinguishing features were cross-referenced with fluorescence responses and authenticated standard reference materials to determine the authenticity and quality grade of the examined samples. Furthermore, the study quantified selected microstructural measurements, such as fiber width and gland distribution, that may be associated with biomechanical properties, including elasticity, structural strength, and tissue resilience. These structural and mechanical characteristics may influence the processing behavior, bioavailability, and pharmacokinetic performance of medicinal plant materials. The results demonstrate that authentic samples possess structurally distinctive and biomechanically robust characteristics, including denser oil chambers in *Aurantii Fructus* and clearly defined spiny pericarp surfaces in *Amomum villosum*, whereas these diagnostic characteristics are absent, less distinct, or substantially diminished in counterfeit counterparts. Image-processing procedures and quantitative morphometric data not only improve visual clarity and identification accuracy but also facilitate a more systematic interpretation of the mechanical behavior and structural integrity of medicinal tissues. Consequently, this integrated approach helps bridge the gap between traditional empirical identification practices and modern scientific validation in the authentication and quality evaluation of TCM materials. By combining micro-morphological microscopy with biomechanical interpretation, the proposed method offers a reliable, cost-effective, accessible, and scalable strategy for frontline pharmacy applications, routine quality grading, professional authentication, and educational training. The findings emphasize the potential relevance of structural and mechanical properties to the therapeutic efficacy and processing performance of herbal materials and provide a foundational methodology for modernizing quality-control protocols within traditional medicine.

Index Terms biomechanical analysis, micro-morphological characteristics, Chinese medicinal materials, authentication, counterfeit materials, pharmacy operations, traditional Chinese medicine

I. Introduction

Traditional Chinese medicine (TCM) has a long-standing history of application in the treatment and prevention of diseases and has formed a cornerstone of medical practice in China and other parts of Asia for thousands of years. The safety, effectiveness, and therapeutic consistency of TCM largely depend on the identity and quality of the medicinal materials used in its preparation [1]–[3]. Ensuring the authenticity, purity, and quality of these materials is therefore essential because counterfeit, adulterated, misidentified, or substandard products may result in ineffective treatment, unexpected adverse effects, inaccurate clinical outcomes, and the erosion of public trust in this valuable system of medicine. This challenge has become increasingly important because the growing demand for Chinese medicinal materials has expanded the market for adulterated, counterfeit, substituted,

or incorrectly identified products. Variations in geographical origin, harvesting time, processing procedures, storage conditions, and commercial handling may also affect the structural characteristics and overall quality of medicinal materials. In this context, the need for precise, reliable, accessible, and efficient identification methods has never been more pressing [4], [5].

Historically, the identification of Chinese medicinal materials has relied heavily on traditional approaches, including visual inspection, olfactory examination, tactile assessment, and other organoleptic tests. Although these techniques remain widely used in pharmaceutical practice, they are subject to several inherent limitations. First, unaided visual inspection may fail to detect subtle morphological characteristics, particularly when complex plant or animal tissues are being examined. Second, traditional identification methods are frequently subjective and highly dependent on the knowledge, practical experience, and observational ability of the pharmacist or technician conducting the assessment. Such dependence may introduce interobserver variability and increase the possibility of identification errors [6], [7]. Furthermore, the increasing availability of sophisticated counterfeit and adulterated materials, some of which closely imitate the color, shape, texture, odor, or external appearance of authentic materials, has further complicated the distinction between genuine medicinal materials and inferior, ineffective, or potentially harmful substitutes.

In response to these challenges, several advanced analytical techniques have been introduced, including physicochemical analysis, chromatographic methods, spectroscopic procedures, and molecular biological approaches. Although these techniques can provide highly accurate and sensitive results, they generally require specialized instrumentation, trained personnel, considerable technical expertise, and time-consuming analytical procedures. Consequently, such techniques are not always suitable for frontline pharmacy operations or rapid routine screening [8]. Moreover, these approaches can be prohibitively expensive and frequently require controlled laboratory environments, standardized reagents, extensive sample preparation, and complicated data interpretation. These requirements make them less practical for routine identification in community pharmacies, educational institutions, and other resource-limited pharmaceutical settings. Therefore, there is a clear need for complementary identification methods that are scientifically informative, operationally efficient, economically accessible, and suitable for implementation in real-world pharmacy environments.

Micro-morphological identification, which involves examining the fine structural characteristics of medicinal materials under magnification, provides a potentially valuable response to these practical limitations. By employing advanced imaging systems, including stereomicroscopes, high-resolution digital cameras, ultraviolet fluorescence imaging, and extended-depth-of-field image synthesis, micro-morphological identification facilitates the visualization and analysis of intricate tissue structures that cannot be clearly observed with the unaided eye. This technique can reveal distinctive characteristics of medicinal materials, including cellular arrangements, surface ornamentation, oil-chamber distribution, glandular structures, fiber organization, vascular patterns, and cell-wall characteristics. These features may serve as reliable diagnostic markers for distinguishing among closely related species, separating authentic materials from counterfeit products, and evaluating differences in material quality. Importantly, micromorphological examination can be relatively cost-effective and straightforward to implement, while producing intuitive visual findings that pharmacy personnel can interpret following appropriate standardized training [9].

Micro-morphological identification may also be considered from a biomechanical perspective because the microscopic organization of biological tissues contributes to their structural integrity and mechanical behavior. Biomechanics is concerned with understanding how biological structures respond to forces and how material properties, including strength, elasticity, stiffness, toughness, and resilience, contribute to their functional behavior. In medicinal plant materials, the organization of cells, fibers, vascular tissues, and cell walls may influence resistance to compression, fracture, deformation, grinding, and other forces encountered during harvesting, processing, storage, and pharmaceutical preparation [9]. For example, cell-wall thickness and fiber arrangement can contribute to the rigidity and resilience of plant tissues. These properties may subsequently influence fragmentation and extraction behavior, although their relationships with the release, absorption, and bioavailability of active compounds require direct experimental verification. Examining these microstructural characteristics can therefore provide useful indirect insights into the structural quality and potential processing performance of Chinese medicinal materials.

It is important, however, to distinguish biomechanical interpretation from direct biomechanical measurement. Microscopic images can demonstrate structural characteristics that may be associated with mechanical behavior, but they cannot independently establish mechanical properties such as elasticity, tensile strength, compressive resistance, or tissue toughness. Confirming such properties would require standardized mechanical testing and statistical evaluation of the relationships between structural measurements and experimentally determined mechanical parameters. Accordingly, the present study employs biomechanical concepts as an interpretive framework for understanding the potential functional significance of observed microstructures rather than treating morphology alone as direct evidence of mechanical performance. This distinction supports a more scientifically cautious interpretation of the potential therapeutic value and quality of Chinese medicinal materials [10].

Furthermore, applying biomechanical principles to micromorphological identification can improve understanding of how medicinal materials behave at the cellular and tissue levels. For instance, the distribution, density, size, and structural integrity of oil chambers are important characteristics for identifying and grading medicinal materials such as *Au-*

rantii Fructus. These characteristics reflect the organization of secretory tissues and the capacity of the material to store oil-containing constituents. Nevertheless, the relationship between oil-chamber morphology and medicinal potency should be confirmed through complementary chemical analyses because morphological abundance does not necessarily provide a direct quantitative measurement of bioactive-compound concentrations. By systematically quantifying and comparing these micro-morphological characteristics, pharmacists and researchers can more rapidly assess the authenticity, structural condition, and potential quality grade of medicinal materials while identifying samples that require further physicochemical, chromatographic, or molecular examination.

Therefore, this study integrates high-resolution micro-morphological observation, ultraviolet fluorescence imaging, extended-depth-of-field synthesis, and quantitative morphometric assessment to examine diagnostically important structural characteristics in selected Chinese medicinal materials. Particular attention is given to oil chambers, surface spines, fibers, glands, cell walls, and other anatomical markers that may differentiate authentic materials from counterfeit or adulterated counterparts. The biomechanical significance of these structural characteristics is interpreted cautiously within the limits of the available morphological evidence. Through this integrated framework, the study seeks to strengthen the scientific basis of routine identification, improve the accessibility of quality-assessment procedures, and support the modernization of authentication practices in frontline pharmacies, pharmaceutical education, and traditional Chinese medicine quality control.

II. Materials

A. Main Instruments

The precision, reliability, and reproducibility of micro-morphological identification depend on the use of appropriate optical instruments, standardized imaging conditions, and suitable image-processing procedures. In the present study, the instrumentation consisted of a stereomicroscope equipped with an SZX-ZB7 adjustable zoom body, a microscope objective lens, a digital imaging system, FCSnap image-processing software, and an ultraviolet illumination system. These instruments were used to observe, photograph, process, and compare the external and internal micro-morphological characteristics of the selected medicinal materials.

The stereomicroscope, equipped with a high-resolution zoom capability and an SZX-ZB7 adjustable zoom body, was used to examine the surfaces and exposed tissue structures of the medicinal materials at different magnification levels. The adjustable zoom mechanism permitted continuous transitions between magnifications and facilitated the observation of both general surface patterns and localized diagnostic structures. These structures included oil chambers, surface spines, fibers, glands, vascular features, and variations in cellular organization. The manufacturer, complete microscope model, magnification range, and numerical aperture were not reported in the available experimental record and should be specified when these details are available.

The microscope objective lens provided the optical resolution required to capture tissue structures used to differentiate authentic samples from their suspected counterfeit counterparts. Before imaging, the lens and microscope settings were adjusted to achieve appropriate focus, field coverage, and illumination. However, the manufacturer, model, magnification, working distance, and other optical specifications of the lens were not documented in the available study materials. Reporting these parameters would improve the reproducibility of the microscopic observations.

A digital imaging system connected to the stereomicroscope was used to capture high-resolution images of the observed micro-morphological characteristics. The captured images preserved visible structural details for subsequent documentation, comparison, and morphometric assessment. To ensure methodological reproducibility, the camera manufacturer, model, sensor resolution, exposure settings, image dimensions, and file format should be reported when this information is available. All comparisons should preferably be conducted using images acquired under equivalent magnification, illumination, exposure, and positioning conditions.

FCSnap imaging software was employed to process and enhance the acquired images. The principal operations included contrast adjustment, image alignment, multilayer merging, and extended-depth-of-field synthesis. Images captured at different focal planes were combined to obtain composite images in which a greater proportion of the specimen surface remained in focus. Image enhancement was used to improve the visibility of existing anatomical structures and was not used to create, remove, or materially alter diagnostic features. The software version and the principal processing parameters should be reported to support the reproducibility of the image-processing workflow.

An ultraviolet illumination system was used to observe the fluorescence characteristics of selected specimens. Ultraviolet fluorescence provided an additional visual characteristic for comparison with the corresponding morphological observations. Nevertheless, fluorescence intensity was not treated as a direct quantitative measurement of oil content, active-compound concentration, biomechanical behavior, or therapeutic efficacy. The wavelength, output intensity, exposure duration, illumination distance, filter configuration, and instrument model were not reported in the available experimental record and should be provided when available because these conditions can substantially influence the appearance and intensity of fluorescence.

No mechanical testing instrument was included in the reported experimental equipment, and no direct tensile, compressive, bending, puncture, fracture, stiffness, elasticity, or toughness tests were performed. Consequently, the microscopic observations obtained using the instruments described above provide morphological and morphometric evidence rather than direct biomechanical measurements. Any discussion of mechanical behavior in this study should therefore be

ARCHIVES DES SCIENCES
A Multidisciplinary Journal

understood as a cautious structural interpretation that requires confirmation through standardized biomechanical testing.

B. Source of Medicinal Materials

The study included medicinal materials obtained from commercial markets, medicinal-material specimen suppliers, pharmacies, and samples of unknown provenance. The recorded sources, identification results, and authenticity classifications of the specimens are presented in Table 1. The collection comprised authentic materials, designated counterfeit materials, and morphologically related substitutes selected for comparative examination. Including specimens from several sources expanded the range of visible characteristics available for comparison; however, the sampling strategy did not constitute a statistically representative survey of the broader Chinese medicinal-material market.

Samples were obtained from the Anguo Medicinal Materials Market, Henan Dingxin Medicinal Material Specimen, Guoyao Bencao Pharmacy, and a community traditional Chinese medicine pharmacy in Shijiazhuang. The Anguo Medicinal Materials Market supplied several materials commonly distributed through commercial medicinal-material channels. Henan Dingxin Medicinal Material Specimen supplied authentic specimens and designated counterfeit or substitute specimens for comparative analysis. Guoyao Bencao Pharmacy and the community traditional Chinese medicine pharmacy supplied materials representative of products encountered in routine pharmacy practice. Several comparison samples had unknown sources, as indicated in Table 1; therefore, no claims concerning their geographical origins, harvesting conditions, processing histories, or storage conditions can be made.

The terms "authentic" and "counterfeit" in Table 1 represent the classifications recorded for the examined samples. To establish these classifications independently, the study should specify the authentication procedure, applicable pharmacopoeial standards, diagnostic reference materials, and qualifications of the person responsible for identification. Where voucher specimens were retained, their voucher numbers and repository information should also be reported. In the absence of these details, the classifications should be interpreted as the recorded identities of the supplied specimens rather than as independently confirmed taxonomic determinations.

The examined materials included *Aurantii Fructus*, three species associated with Amomum materials, *Atractylodis Rhizoma*, *Ziziphi Spinosae Semen*, *Carthami Flos*, *Plantaginis Semen*, *Euodiae Fructus*, *Perillae Fructus*, and *Sinapis Semen*. Designated counterfeit or substitute samples included *Amomum gagnepainii*, *Atractylodes japonica*, *Vicia lens*, *Ziziphus mauritiana*, and a weight-increased sample of *Carthami Flos*. Sample identifiers were retained throughout preparation, imaging, processing, measurement, and comparison to prevent confusion among authentic samples and their corresponding counterfeit or substitute materials.

Micro-morphological characteristics such as cell-wall appearance, oil-chamber distribution, surface ornamentation, fiber organization, and tissue arrangement were examined as diagnostic structural features. Although these characteristics may be associated with the physical behavior of plant tissues, microscopy alone cannot establish cellulose or lignin content, mechanical resilience, tensile strength, elasticity, or structural toughness. Determination of chemical composition would require appropriate chemical analyses, whereas confirmation of mechanical properties would require standardized biomechanical experiments.

Similarly, ultraviolet fluorescence was used as a comparative optical response and not as direct evidence of biomechanical stress, secondary-metabolite concentration, or therapeutic potency. For example, the distribution and density of visible oil chambers in *Aurantii Fructus* may assist morphological identification, but the images alone cannot demonstrate the concentration or pharmacological activity of the compounds contained within those structures. Such relationships would require complementary chromatographic, spectroscopic, pharmacological, and statistical analyses.

Accordingly, the selected instruments and diverse sample sources supported a comparative micro-morphological assessment of the medicinal materials. The resulting observations may provide useful information for routine authentication and quality screening in pharmaceutical and educational environments. However, the present materials permit only morphological and morphometric comparisons; they do not independently demonstrate biomechanical performance, chemical composition, bioavailability, pharmacokinetic behavior, or therapeutic efficacy.

Table 1: Sources, recorded identities, and authenticity classifications of the examined medicinal-material samples.

No.	Source of medicinal material	Recorded identification	Classification
1a	Anguo Medicinal Materials Market	Aurantii Fructus	Authentic
1b	Henan Dingxin Medicinal Material Specimen	Aurantii Fructus	Authentic
1c	Guoyao Bencao Pharmacy	Aurantii Fructus	Authentic
2a	Henan Dingxin Medicinal Material Specimen	*Amomum longiligulare* T. L. Wu	Authentic
2b	Henan Dingxin Medicinal Material Specimen	*Amomum gagnepainii* T. L. Wu et al.	Counterfeit
2c	Henan Dingxin Medicinal Material Specimen	*Amomum villosum* Lour.	Authentic
3a	Community Traditional Chinese Medicine Pharmacy, Shijiazhuang	Atractylodis Rhizoma	Authentic
3b	Unknown	*Atractylodes japonica* Koidz. ex Kitam.	Counterfeit
4a	Anguo Medicinal Materials Market	Ziziphi Spinosae Semen	Authentic
4b	Unknown	*Vicia lens*	Counterfeit
4c	Unknown	*Ziziphus mauritiana*	Counterfeit
5a	Guoyao Bencao Pharmacy	Carthami Flos	Authentic
5b	Unknown	Weight-increased Carthami Flos	Counterfeit
6	Guoyao Bencao Pharmacy	Plantaginis Semen	Authentic
7	Anguo Medicinal Materials Market	Euodiae Fructus	Authentic
8	Anguo Medicinal Materials Market	Perillae Fructus	Authentic
9	Anguo Medicinal Materials Market	Sinapis Semen	Authentic

III. Methods

A. Study Design

This study employed a comparative, descriptive imaging design to examine the visible micro-morphological characteristics of selected authentic and designated counterfeit Chinese medicinal materials. The analytical workflow consisted of sample preparation, stereomicroscopic observation, digital photography, extended-depth-of-field (EDF) image synthesis, image processing, morphometric examination, and comparison with the recorded characteristics of reference specimens. The study was designed primarily to evaluate the usefulness of micro-morphological features for material identification. No direct mechanical, chemical, pharmacological, bioavailability, or pharmacokinetic tests were conducted. Consequently,

ARCHIVES DES SCIENCES
A Multidisciplinary Journal

biomechanical implications were considered only as cautious interpretations of the observed structural characteristics and not as experimentally verified mechanical properties.

B. Preparation of Medicinal Materials

Each medicinal-material specimen was assigned and recorded using the sample identification number provided in Table 1. These identifiers were retained throughout sample preparation, observation, photography, image processing, measurement, and comparative identification to reduce the possibility of specimen misclassification.

Before microscopic examination, loose dust and superficial debris were carefully removed from each sample using a clean, soft brush. No chemical cleaning agents, solvents, stains, mounting media, or destructive pretreatments were applied because these procedures could alter the natural color, fluorescence, texture, or surface morphology of the specimens. The samples were examined in their available commercial or specimen form.

A background color that provided sufficient visual contrast with the color of each specimen was selected before photography. The choice of background was intended to improve the visibility of specimen boundaries and surface characteristics without modifying the appearance of the material itself. Each sample was positioned at different orientations so that multiple regions of its external surface could be examined. Where relevant, the specimen was rotated to expose diagnostically important structures, including ridges, depressions, surface spines, oil chambers, fibers, glands, seed-coat patterns, and other visible anatomical characteristics.

C. Observation and Photography of Medicinal Materials

Before observation and photography, the stereomicroscope, digital imaging system, FCSnap software, and LED illumination source were activated and checked. The camera and light-source settings were adjusted to obtain adequate brightness, contrast, and color representation. The specimen was then positioned beneath the microscope, and the focus was adjusted until the target surface region could be visualized clearly.

The microscope zoom body was adjusted according to specimen size and the dimensions of the morphological feature being examined. Images were acquired at nominal zoom settings of $\times 0.8$, $\times 1$, $\times 1.25$, $\times 1.6$, or $\times 2$, as appropriate. These values represent microscope zoom settings rather than complete optical magnifications because the total magnification also depends on the objective lens, eyepiece, camera adapter, and digital acquisition configuration.

For EDF image acquisition, the fine-focus control was progressively moved through the vertical extent of the region of interest. Image capture began when the uppermost relevant structures entered focus and continued across successive focal planes until the target structures passed out of focus. Depending on the depth and structural complexity of the specimen surface, between 5 and 30 images were acquired for an individual focal stack. Successive images were obtained from approximately the same field of view while different depth planes were brought into focus.

The image stacks were synthesized using EDF processing to produce composite images containing a greater depth of visibly focused structure than could be obtained from a single exposure. The resulting composites were used to examine diagnostically relevant surface and tissue characteristics. EDF synthesis improved the visibility of structures located at different focal depths; however, it did not provide direct three-dimensional measurements of tissue volume, mechanical behavior, chemical composition, or therapeutic activity.

Ultraviolet illumination was used for specimens requiring fluorescence examination. Images obtained under ultraviolet illumination were evaluated separately from those acquired under visible LED illumination. Fluorescence was recorded as a comparative optical characteristic only. Because instrument wavelength, output intensity, exposure duration, filter configuration, and illumination distance were not available in the experimental record, fluorescence intensity was not treated as a calibrated quantitative variable or as direct evidence of a specific chemical constituent.

D. Image Processing

The acquired image sets were imported into FCSnap software for organization, enhancement, alignment, and EDF synthesis. Images from different specimens, magnifications, illumination conditions, and fields of view were maintained as separate sets to prevent inappropriate merging or direct comparison of images acquired under non-equivalent conditions.

Initial processing involved adjustment of image contrast and brightness to improve the visibility of existing micromorphological features, including cell-wall patterns, oil-chamber boundaries, surface projections, glandular structures, and fiber arrangements. Adjustments were applied conservatively so that the underlying diagnostic structures were not created, deleted, displaced, or materially altered. Images intended for direct comparison were processed using equivalent settings whenever the available acquisition conditions permitted such standardization.

Images belonging to the same focal stack were aligned using displacement and scaling functions. Alignment was performed to compensate for small positional differences introduced during focusing and to maintain the relative proportions of the observed structures. Images obtained at different microscope zoom settings were not merged into a single morphometric dataset unless their spatial scales could be independently established.

Following alignment, the focal layers were combined using the EDF function. The software selected or integrated sharply focused regions from the successive focal planes to produce a composite image with an expanded visible depth of field. Each composite was visually inspected for alignment errors, duplicated boundaries, halos, discontinuities, or other processing artifacts. Where processing artifacts could interfere with interpretation, the corresponding original focal images were consulted.

ARCHIVES DES SCIENCES
A Multidisciplinary Journal

Image processing was employed to improve visualization and documentation rather than to generate direct biomechanical measurements. Fiber thickness, cellular organization, cell-wall appearance, and tissue arrangement may have structural relevance, but the processed images alone cannot determine elasticity, stiffness, toughness, tensile strength, compressive resistance, or fracture behavior. Such properties would require calibrated mechanical testing under controlled loading conditions.

E. Sample Measurement

Morphometric examination was undertaken to document measurable dimensions of selected microstructural characteristics. Each specimen was positioned beneath the microscope objective so that the target region remained stable and clearly visible. The zoom body was adjusted to the required nominal setting of $\times 0.8$, $\times 1$, $\times 1.25$, $\times 1.6$, or $\times 2$, and the fine-focus control was used to obtain a sharply defined image of the feature selected for measurement.

The measuring-ruler function available in FCSnap was used to examine the apparent length, width, diameter, spacing, or distribution of visible structures, including oil chambers, fibers, surface projections, and cellular arrangements. Measurements were made only from images in which the boundaries of the target structure could be identified with sufficient clarity. The corresponding specimen identifier, field of view, zoom setting, and structural feature were retained with the image record to facilitate comparison.

Accurate dimensional measurements require spatial calibration of the imaging system at every optical configuration. The available experimental record did not specify the use of a stage micrometer, calibration standard, pixel-to-length conversion factor, measurement uncertainty, number of replicate fields, or number of repeated measurements. Therefore, any measurements obtained from the ruler tool should be interpreted as descriptive morphometric observations rather than fully validated quantitative measurements. Comparisons between images acquired at different zoom settings should not be considered metrically equivalent unless the corresponding calibration factors are available.

High-resolution images were retained to document the measured structures and support comparison among authentic and designated counterfeit specimens. Because the study did not report independent replicate counts or a predefined statistical sampling procedure, the analysis was descriptive. No inferential statistical tests, confidence intervals, interobserver agreement estimates, diagnostic sensitivity values, diagnostic specificity values, or classification-accuracy measures were calculated.

From a biomechanical perspective, the dimensions and organization of microstructures may generate hypotheses concerning the physical behavior of medicinal tissues. For example, fiber arrangement and cell-wall thickness may be associated with resistance to deformation or fragmentation. Nevertheless, the dimensions of oil chambers or fibers cannot independently establish a plant's resistance to environmental stress, the release of bioactive compounds, bioavailability, or therapeutic efficacy. Establishing these relationships would require direct mechanical testing, quantitative chemical analysis, extraction experiments, and appropriate statistical correlation.

F. Micro-Morphological Identification

Micro-morphological identification was performed through systematic description and comparison of the visible characteristics documented during stereomicroscopic observation, fluorescence examination, image processing, and morphometric assessment. The analysis focused on structures that could be consistently recognized in the acquired images, including overall surface configuration, color distribution, ridges, depressions, spines, glandular structures, oil chambers, fibers, cellular patterns, and cell-wall appearance.

For *Aurantii Fructus*, particular attention was directed toward the presence, apparent density, distribution, size, and position of oil chambers near the outer region of the material. These characteristics were compared among samples 1a, 1b, and 1c. For the Amomum-related materials, the shape, density, prominence, and arrangement of surface spines or projections were examined and compared among samples 2a, 2b, and 2c. Corresponding diagnostic characteristics were examined for the remaining authentic and designated counterfeit materials according to the visible structures present in each specimen.

The observed characteristics were compared with those of specimens recorded as authentic reference materials and with the identities and classifications listed in Table 1. Deviations in surface ornamentation, oil-chamber distribution, tissue organization, cellular appearance, and other diagnostic characteristics were documented. Because the available protocol did not report blinded evaluation, independent assessors, voucher-specimen numbers, molecular confirmation, chromatographic confirmation, or formal pharmacopoeial authentication criteria, the resulting identifications represent comparative morphological assessments rather than independently validated taxonomic determinations.

The possible functional significance of the observed structures was interpreted conservatively. A greater apparent density of oil chambers may indicate a difference in the abundance or organization of secretory tissues, but it does not directly demonstrate a higher volatile-oil concentration or greater therapeutic efficacy. Likewise, thicker-appearing cell walls or more orderly fiber arrangements may suggest differences in tissue construction, but they do not directly establish superior structural integrity, extraction efficiency, absorption, or biomechanical performance.

Accordingly, the method integrated standardized specimen labeling, surface preparation, stereomicroscopic observation, multifocal photography, EDF synthesis, conservative image enhancement, descriptive morphometry, and comparison with recorded reference specimens. This workflow provides a practical approach to preliminary authentication and quality screening of Chinese medicinal materials. Its findings should be interpreted as morphological evidence that may guide

ARCHIVES DES SCIENCES
A Multidisciplinary Journal

subsequent confirmatory testing rather than as direct proof of chemical composition, mechanical properties, pharmacokinetic performance, clinical suitability, or therapeutic potency.

IV. Results

A. Identification of Aurantii Fructus

Aurantii Fructus is the dried immature fruit of *Citrus aurantium* L. and its cultivated varieties in the family Rutaceae. The prepared material commonly consists of irregular, arc-shaped slices characterized by one or two rows of punctate oil chambers near the outer edge [4]. These oil chambers represent an important morphological feature for the identification and comparative assessment of Aurantii Fructus.

The peripheral regions of samples 1a, 1b, and 1c were examined at a nominal microscope zoom setting of $\times 0.8$. As shown in Figure 1, sample 1a contained a relatively sparse row of visible oil chambers, sample 1b displayed an intermediate distribution, and sample 1c exhibited comparatively dense oil chambers arranged near the outer margin. These differences provided readily visible criteria for comparing the three samples under equivalent observational conditions.

Ultraviolet examination at 365 nm revealed differences in the visible fluorescence responses of the three Aurantii Fructus samples, as presented in Figure 2. Samples with more prominent oil-chamber structures appeared to display stronger fluorescence under the applied imaging conditions. Nevertheless, fluorescence intensity was not quantitatively calibrated, and the chemical composition of the fluorescing regions was not independently determined. Therefore, the observed fluorescence cannot by itself demonstrate volatile-oil concentration, therapeutic potency, or quality grade. The combined visible-light and ultraviolet observations provide comparative morphological evidence that may support preliminary identification, but any relationship with volatile-oil content requires confirmation through quantitative chemical analysis.

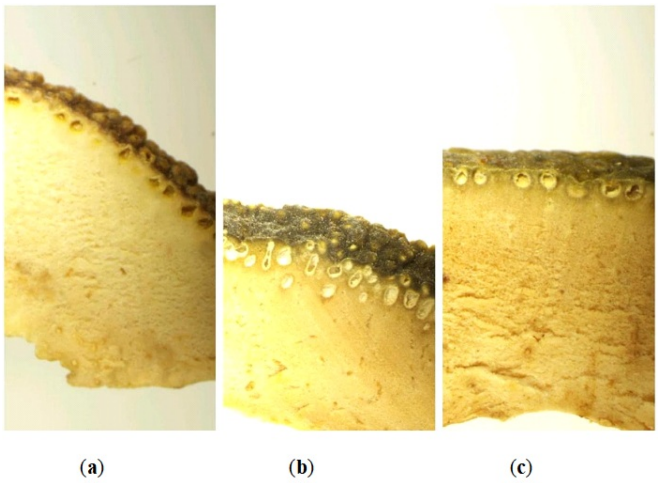

Figure 1: Micro-morphological characteristics of Aurantii Fructus observed at a nominal zoom setting of $\times 0.8$: (a) sample 1a from the Anguo Medicinal Materials Market; (b) sample 1b from Henan Dingxin Medicinal Material Specimen; and (c) sample 1c from Guoyao Bencao Pharmacy.

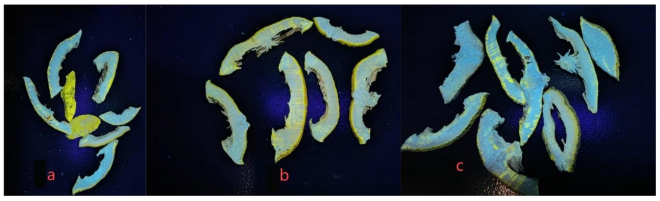

Figure 2: Ultraviolet fluorescence characteristics of Aurantii Fructus observed at 365 nm: (a) sample 1a from the Anguo Medicinal Materials Market; (b) sample 1b from Henan Dingxin Medicinal Material Specimen; and (c) sample 1c from Guoyao Bencao Pharmacy.

B. Identification of Amomum Materials

In the pharmacognostic nomenclature used in this study, Amomum medicinal materials belong to the family Zingiberaceae and include dried mature fruits associated with *Amomum villosum* Lour., *Amomum villosum* var. *xanthioides* T. L. Wu & Senjen, and *Amomum longiligulare* T. L. Wu. Because several related taxa and morphologically similar commercial substitutes are encountered in the medicinal-material market, accurate differentiation requires examination of multiple external and micro-morphological characteristics rather than reliance on color alone.

Three Amomum-related specimens were compared: sample 2a, identified as Hainan Amomum (*Amomum longiligulare* T. L. Wu); sample 2b, identified as *Amomum gagnepainii* T. L. Wu et al. and classified in this study as a counterfeit or substitute; and sample 2c, identified as Yangchun Amomum (*Amomum villosum* Lour.). The recorded classification of each specimen is provided in Table 1. The comparative observations focused on fruit color, overall shape, longitudinal ridges, surface projections, seed shape, seed-coat texture, aroma, and taste.

1) Macroscopic characteristics

The external pericarps of all three specimens were brown, and no sufficiently distinctive color difference was observed to permit reliable identification based solely on this characteristic. Differences were evident, however, in fruit shape and ridge prominence. The Hainan Amomum and *A. gagnepainii* specimens were comparatively elongated and predominantly ovoid, whereas the Yangchun Amomum specimen was shorter and more broadly ovoid. The Hainan Amomum specimen displayed three relatively distinct longitudinal ridges. By comparison, the ridges of the Yangchun Amomum and *A. gagnepainii* specimens were less prominent and comparatively blunt.

2) Micro-morphological characteristics

The surface characteristics of the three specimens are compared in Figure 3. Under the stereomicroscope, Yangchun Amomum and *A. gagnepainii* displayed fine longitudinal pro-

ARCHIVES DES SCIENCES
A Multidisciplinary Journal

jections distributed across the fruit surface, whereas these structures were less pronounced in the Hainan Amomum specimen. The surface of Yangchun Amomum was densely covered with relatively sharp, spine-like projections. In contrast, the *A. gagnepainii* specimen contained fewer and more sparsely distributed spines, while the Hainan Amomum specimen exhibited larger, flatter, and more recumbent projections. These differences in spine density, shape, orientation, and distribution constituted the most readily distinguishable surface characteristics among the three specimens.

The seed characteristics are presented in Figure 4. Seeds from all three specimens were predominantly brown, although some seeds of the Hainan Amomum specimen exhibited a reddish-brown coloration. Hainan Amomum seeds were generally ovoid and displayed subtle undulating projections together with visible longitudinal striations. By contrast, the seeds of *A. gagnepainii* and Yangchun Amomum were more irregularly polyhedral and possessed comparatively prominent undulating surface textures. Light-brown membranous structures resembling a pseudopericarp were also visible on portions of these seeds.

3) Sensory characteristics

Differences were additionally recorded in aroma and taste. Yangchun Amomum possessed a comparatively strong aromatic odor and a spicy, cooling, and slightly bitter taste. The Hainan Amomum and *A. gagnepainii* specimens exhibited milder aromas and less pronounced flavors. These sensory characteristics may supplement morphological examination, but they remain subjective and should not be used as the sole basis for authentication.

Taken together, Figures 3 and 4 demonstrate that the three specimens could be differentiated more effectively through the combined examination of fruit shape, ridge prominence, surface-spine morphology, seed shape, and seed-coat texture than through external color alone. The findings remain descriptive because diagnostic sensitivity, specificity, classification accuracy, interobserver agreement, and chemical confirmation were not determined.

Figure 3: Comparative micro-morphological characteristics of Amomum fruit surfaces observed at a nominal zoom setting of $\times 0.8$: (a) Hainan Amomum, *Amomum longiligulare* T. L. Wu (sample 2a); (b) *Amomum gagnepainii* T. L. Wu et al. (sample 2b); and (c) Yangchun Amomum, *Amomum villosum* Lour. (sample 2c).

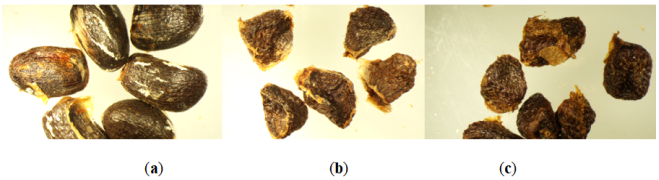

Figure 4: Comparative micro-morphological characteristics of Amomum seeds observed at a nominal zoom setting of $\times 1$: (a) Hainan Amomum, *Amomum longiligulare* T. L. Wu (sample 2a); (b) *Amomum gagnepainii* T. L. Wu et al. (sample 2b); and (c) Yangchun Amomum, *Amomum villosum* Lour. (sample 2c).

C. Identification of Atractylodis Rhizoma

Atractylodis Rhizoma is a medicinal material derived from the dried rhizome of plants belonging to the genus *Atractylodes* in the family Asteraceae. The authentic specimen examined in this study was compared with *Atractylodes japonica* Koidz. ex Kitam., which was designated as a counterfeit or substitute specimen in Table 1.

As illustrated in Figure 5, the *A. japonica* specimen exhibited a predominantly grayish-white cut surface, relatively few cinnabar-colored spots, less conspicuous oil chambers, and light-brown peripheral regions. In comparison, the authentic Atractylodis Rhizoma specimen displayed a yellowish-white surface, numerous reddish-brown oil-chamber centers, orange-red peripheral regions, and a characteristic aromatic odor. The abundance and coloration of the visible oil chambers, together with the overall color of the cut surface, provided useful characteristics for differentiating the two examined specimens.

These observations demonstrate the potential value of stereomicroscopic examination for recognizing visible differences between Atractylodis Rhizoma and the designated substitute. However, the observed oil-chamber characteristics do not independently establish the chemical composition, concentration of active compounds, or therapeutic quality of either specimen.

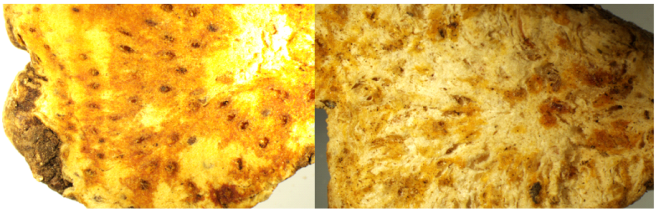

Figure 5: Comparative micro-morphological characteristics observed at a nominal zoom setting of $\times 0.8$: (a) authentic Atractylodis Rhizoma (sample 3a); and (b) *Atractylodes japonica* Koidz. ex Kitam. (sample 3b), designated as a counterfeit or substitute specimen.

ARCHIVES DES SCIENCES
A Multidisciplinary Journal

D. Identification of Ziziphi Spinosae Semen

Ziziphi Spinosae Semen is the dried mature seed of *Ziziphus jujuba* Mill. var. *spinosa* (Bunge) Hu ex H. F. Chou, a member of the family Rhamnaceae. The authentic material was compared with processed *Vicia lens* and *Ziziphus mauritiana*, both of which were designated as counterfeit or substitute specimens in Table 1.

The authentic Ziziphi Spinosae Semen specimen was flattened and nearly circular to broadly ovoid, with both surfaces slightly convex. One surface possessed a raised longitudinal ridge through the central region, whereas the opposite surface was comparatively smooth and slightly protruding. The seed coat was smooth, glossy, and purplish-brown.

The processed *Vicia lens* specimen was also flattened and approximately circular, but it lacked a clearly pointed end. One surface was slightly convex, the seed coat was wrinkled, and the overall form was flatter than that of authentic Ziziphi Spinosae Semen. Its coloration ranged from reddish-brown to brown and was unevenly distributed. Some regions displayed visible color halos consistent with artificial processing or dyeing.

The *Ziziphus mauritiana* specimen was flattened and approximately circular, with one comparatively blunt end and one more pointed end. One surface was convex, while the opposite surface was relatively flat. Its coloration was heterogeneous and included visible reddish-brown mottling.

The side-by-side comparison in Figure 6 shows that overall shape, terminal configuration, surface convexity, seed-coat texture, gloss, and color uniformity can assist in differentiating authentic Ziziphi Spinosae Semen from the two designated counterfeit specimens. These characteristics support preliminary morphological screening, although definitive authentication would require comparison with validated reference materials and, where necessary, complementary chemical or molecular testing.

(a) (b) (c)

Figure 6: Comparative micro-morphological characteristics observed at a nominal zoom setting of $\times 1$: (a) authentic Ziziphi Spinosae Semen (sample 4a); (b) processed *Vicia lens* (sample 4b); and (c) *Ziziphus mauritiana* (sample 4c).

E. Identification of Carthami Flos

Carthami Flos is the dried flower of *Carthamus tinctorius* L., which belongs to the family Asteraceae. The authentic specimen was compared with a commercially weight-increased specimen designated as counterfeit in Table 1.

As shown in Figure 7, authentic Carthami Flos consisted predominantly of recognizable tubular florets with reddish-yellow to red surfaces. The corolla tubes were slender and comparatively intact, and yellow pollen grains were visible on portions of the floral structures. In contrast, the weight-increased specimen was fragmented and incomplete. Its corolla and staminal structures were less distinct, and portions of the floral material appeared bonded into clusters by the added weighting substance.

The comparison in Figure 7 indicates that floret integrity, visibility of the corolla and stamens, pollen retention, fragmentation, and aggregation can assist in detecting this form of adulteration. Microscopic observation can reveal the physical presence and distribution of added material, but it does not determine its chemical identity or quantify the degree of adulteration. Such determinations would require additional chemical and gravimetric analyses.

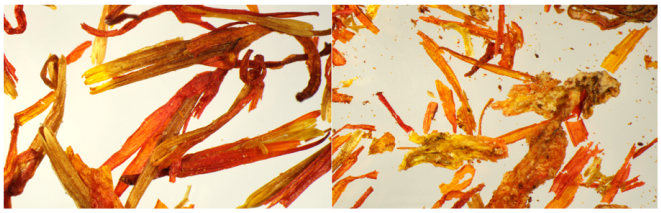

(a) (b)

Figure 7: Comparative micro-morphological characteristics of Carthami Flos observed at a nominal zoom setting of $\times 1$: (a) authentic Carthami Flos (sample 5a); and (b) adulterated, weight-increased Carthami Flos (sample 5b).

F. Identification of Common Small-Seed Medicinal Materials

Several small-seed medicinal materials were examined to determine whether stereomicroscopic imaging could make their diagnostically relevant surface characteristics more readily visible. The observations for Plantaginis Semen, Euodiae Fructus, Perillae Fructus, and Sinapis Semen are presented in Figures 8–11, respectively.

1) Identification of Plantaginis Semen

Plantaginis Semen consists of the dried mature seeds of *Plantago asiatica* L. or *Plantago depressa* Willd. The examined seeds were irregularly oblong or triangular-oblong, slightly flattened, approximately 2 mm long, and approximately 1 mm wide. Their coloration ranged from yellowish-brown to blackish-brown, and their surfaces exhibited fine wrinkles.

The enlarged views in Figure 8 reveal a granular surface texture that was less apparent without magnification. A grayish-white concave region, corresponding to the hilum, was visible on one side of the seed. Comparison of panels (a) and (b) demonstrates how increased zoom improved the visibility of the fine surface wrinkles, granular texture, and concave hilar region. These characteristics provide practical morphological criteria for recognizing Plantaginis Semen during preliminary examination.

ARCHIVES DES SCIENCES
A Multidisciplinary Journal

(a) (b)

Figure 8: Micro-morphological characteristics of *Plantago asiatica* seeds: (a) nominal zoom setting of $\times 1.25$; and (b) nominal zoom setting of $\times 2.5$.

2) Identification of Euodiae Fructus

Euodiae Fructus consists of dried, nearly mature fruits of plants traditionally recorded under the pharmacognostic name *Evodia rutaecarpa* (Juss.) Benth. and its recognized varieties. The examined fruits were pentagonal and oblate-spherical, with diameters ranging from approximately 2 to 5 mm. Their coloration ranged from yellowish-green to brown.

As presented in Figure 9, the apical region was concave and displayed conspicuous pentagonal, star-shaped dehiscence lines. The fruit surface was uneven and wrinkled, with folds resembling intestinal convolutions, together with punctate projections or depressed oil spots. In some specimens, a residual fruit stalk remained attached at the base and was covered with yellowish trichomes. The material possessed a strong aromatic odor and a bitter, pungent taste.

Panels (a) and (b) of Figure 9 show the overall shape and surface ornamentation at different zoom settings, while panel (c) displays the residual fruit stalk. The combination of pentagonal form, apical star-shaped divisions, wrinkled surface, punctate oil spots, and occasional stalk remnants provided a recognizable set of diagnostic characteristics.

(a) (b) (c)

Figure 9: Micro-morphological characteristics of Euodiae Fructus: (a) overall fruit morphology at a nominal zoom setting of $\times 1$; (b) surface characteristics at $\times 2.5$; and (c) residual fruit stalk at $\times 1.6$.

3) Identification of Perillae Fructus

Perillae Fructus is the dried mature fruit of *Perilla frutescens* (L.) Britton, a member of the family Lamiaceae. The examined fruits were approximately spherical to broadly ovoid and measured about 1.5 mm in diameter. Their surfaces were grayish-brown and displayed conspicuous dark-purple reticulation.

As shown in Figure 10, the reticulate ridges were slightly elevated and formed irregular polygonal compartments. The fruit base was slightly pointed and contained a grayish-white punctate stalk scar. This scar displayed a pale, approximately circular outer margin and a grayish-black center. The pericarp was thin and brittle, and several fruits were cracked, revealing a yellowish-white kernel. When crushed, the material released a characteristic aromatic odor and possessed a mildly pungent taste.

The images in Figure 10 demonstrate that increased magnification improved the visibility of the polygonal reticulation and stalk scar. Panel (a) presents the general fruit morphology, panel (b) shows the reticulate surface in greater detail, and panel (c) emphasizes the stalk-mark region.

(a) (b) (c)

Figure 10: Micro-morphological characteristics of Perillae Fructus derived from *Perilla frutescens* (L.) Britton: (a) overall fruit morphology at a nominal zoom setting of $\times 1.25$; (b) reticulate surface characteristics at $\times 2$; and (c) stalk-mark region at $\times 2$.

4) Identification of Sinapis Semen

Sinapis Semen is associated with the dried mature seeds of *Sinapis alba* L. or related mustard materials, including *Brassica juncea* (L.) Czern. & Coss., in the family Brassicaceae. The specimen examined in the present study was recorded as white Sinapis Semen. It was approximately spherical, light yellow, and 1.5–2.5 mm in diameter.

Figure 11 shows that the seed surface possessed fine reticulation and an orange-peel-like punctate texture. A distinct, point-like hilum was also visible and was surrounded by pale, fine, hair-like material. The specimen possessed a mild odor and a distinctly pungent taste.

Panels (a) and (b) of Figure 11 present the overall seed form and reticulate surface at nominal zoom settings of $\times 1.25$ and $\times 2$, respectively, while panel (c) highlights the hilar region. The combination of seed size, light-yellow coloration, finely reticulate surface, punctate texture, and distinct hilum constituted the principal characteristics recorded for this specimen.

(a) (b) (c)

Figure 11: Micro-morphological characteristics of white Sinapis Semen: (a) overall seed morphology at a nominal zoom setting of $\times 1.25$; (b) reticulate and punctate surface characteristics at $\times 2$; and (c) detailed appearance of the hilar region.

G. Summary of Comparative Findings

The comparative observations demonstrated that stereomicroscopy and EDF-supported digital imaging made several diagnostically relevant characteristics more readily visible. These included the marginal oil chambers of Aurantii Fructus, the surface-spine patterns and seed textures of the Amomum materials, the colored oil-chamber regions of Atractylodis Rhizoma, the seed-coat characteristics of Ziziphi Spinosae Semen and its designated substitutes, and the structural disruption associated with weight-increased Carthami Flos. The surface reticulation, hilar regions, stalk scars, and residual stalk structures of the smaller medicinal materials were also documented in Figures 8–11.

All figures in this section present descriptive observations from the examined specimens. The images support preliminary morphological differentiation but do not establish diagnostic accuracy across broader commercial populations. Furthermore, the observations do not directly measure biomechanical properties, chemical composition, volatile-oil concentration, pharmacokinetic behavior, bioavailability, or therapeutic efficacy. Confirmation of these relationships would require replicated sampling, validated authentication standards, calibrated morphometry, quantitative chemical assays, direct mechanical testing, and appropriate statistical analysis.

V. Conclusion

This study demonstrates the practical feasibility and potential utility of stereomicroscopic observation, ultraviolet fluorescence imaging, extended-depth-of-field synthesis, and descriptive morphometric examination for the preliminary authentication and comparative quality assessment of traditional Chinese medicinal materials. The imaging workflow made diagnostically relevant surface and tissue characteristics more clearly visible and facilitated structured comparisons between specimens recorded as authentic and those designated as counterfeit, adulterated, or substitute materials.

The comparative results indicate that anatomical characteristics such as the apparent density and distribution of oil chambers, the shape and arrangement of surface spines, seed-coat patterns, surface microtexture, hilar characteristics, and the integrity of floral structures can provide useful markers for distinguishing the examined specimens. These characteristics were particularly informative for comparing Aurantii Fructus, Amomum materials, Atractylodis Rhizoma, Ziziphi Spinosae Semen, Carthami Flos, and several common small-seed medicinal materials. The findings therefore support the use of micro-morphological imaging as an accessible and comparatively economical method for preliminary screening, routine pharmacy examination, and educational training.

However, the present findings do not establish that the examined materials were differentiated with high diagnostic precision because sensitivity, specificity, classification accuracy, interobserver agreement, and measurement uncertainty were not evaluated. In addition, ultraviolet fluorescence was assessed descriptively and was not calibrated against the concentrations of volatile oils or other chemical constituents. The authenticity classifications were based on the recorded identities of the supplied specimens and were not independently confirmed through molecular, chromatographic, or other validated analytical procedures.

Although the observed microstructures may have potential mechanical or functional significance, this study did not directly measure elasticity, stiffness, strength, toughness, resilience, fracture resistance, or other biomechanical properties. Accordingly, oil-chamber density, epidermal-spine arrangement, fiber organization, cell-wall appearance, and surface microtexture should not be interpreted as direct evidence of biomechanical performance, bioavailability, pharmacokinetic behavior, therapeutic potency, or clinical efficacy. These structural observations provide hypotheses for subsequent investigation rather than confirmation of causal structural–mechanical or structural–pharmacological relationships.

Future studies should incorporate larger and independently authenticated sample sets, voucher specimens, standardized image-acquisition conditions, spatial calibration, replicate measurements, blinded evaluation, and formal statistical analysis. Direct mechanical testing should also be combined with quantitative chemical assays to determine whether specific micro-morphological characteristics are associated with mechanical behavior, active-compound concentration, extraction performance, or other validated indicators of medicinal-material quality. Subject to these limitations, the present approach provides a useful foundation for developing more objective and reproducible micro-morphological protocols for the preliminary authentication of traditional Chinese medicinal materials.

Availability of Data and Materials

The images, measurements, and other data supporting the findings of this study are available from the corresponding author upon reasonable request.

Ethical Approval

Not applicable. This study examined commercially obtained and reference medicinal-material specimens and did not involve human participants, human biological materials, live vertebrate animals, or identifiable personal data.

Conflict of Interest

The author declares no conflict of interest.

References

[1] Yang, D. (2024). Application of micro-morphological identification in the quality evaluation of Chinese medicine [In Chinese]. *Special Economic Animals and Plants, 27*(2), 167–171.

[2] Zhang, L., Lou, Z., Zhu, X., Chen, Y., Zhu, J., & Huang, L. (2024). Application of micro-macroscopical identification in quality acceptance of Chinese herbal pieces in medical institutions [In Chinese]. *Chinese Pharmacist, 27*(8), 1309–1319.

[3] Zhou, J., & Yang, Q. (2011). Microscopic characteristics identification of Chinese materia medica [In Chinese]. *Journal of Anhui Traditional Chinese Medical College, 30*(1), 66–68.

[4] Chinese Pharmacopoeia Commission. (2020). *Pharmacopoeia of the People's Republic of China: 2020 edition (Vol. 1)* [In Chinese]. China Medical Science Press.

[5] Li, F., Zhou, R., & Liu, Q. (2018). Micro-morphological identification of *Lysimachia christinae* and its adulterants [In Chinese]. *Strait Pharmaceutical Journal, 30*(7), 39–41.
[6] Li, F., Liu, Q., & Zhao, Y. (2018). Comparative study of the micro-morphological characteristics of *Lysimachia christinae* and *Lysimachia congestiflora* [In Chinese]. *Inner Mongolia Journal of Traditional Chinese Medicine, 37*(11), 97–98.
[7] Hu, X., Yuan, W., Wang, J., Chen, W., Wang, S., & Wang, Y. (2021). Identification of microscopic characteristics of *Amomum villosum* from different habitats and its adulterants [In Chinese]. *China Pharmacy, 32*(5), 590–594.
[8] Hou, F., Guo, L., Song, J., Zhang, D., Zheng, K., Zheng, Y., & Wang, Q. (2019). Identification of Amomi Fructus and its adulterate products by characteristic and micro-morphological features in the Hebei Anguo market [In Chinese]. *Journal of Nanjing University of Chinese Medicine, 35*(2), 214–217.
[9] Ju, K., Xia, D., Wang, F., Ma, J., & Zhou, J. (2023). Micro-morphological identification of *Gynostemma pentaphyllum* and *Cayratia japonica* [In Chinese]. *Journal of Jiangxi University of Traditional Chinese Medicine, 35*(6), 89–91, 97.
[10] Zou, L., Yi, D., Pan, Y., Lin, L., Xiao, C., Pei, G., Xue, J., & Liu, X. (2024). Micro-characteristics and microscopic identification of nine kinds of *Epimedium* leaves [In Chinese]. *Chinese Pharmaceutical Journal, 59*(9), 776–788.
[11] Hou, F., Lin, X., Fan, W., Yang, Y., Zheng, Y., & Sun, B. (2025). Micro-morphological identification of the bones and scales of *Bungarus multicinctus* and its adulterants [In Chinese]. *Journal of Liaoning University of Traditional Chinese Medicine, 27*(5), 42–46, 221.
[12] Liang, Q., Ouyang, M., Chen, B., Liang, L., Chen, H., Che, W., Luo, X., & Zhang, X. (2023). Comparison of differences in micro-morphological and microscopic identification between *Lonicerae Japonicae Flos* and *Lonicerae Flos* [In Chinese]. *Strait Pharmaceutical Journal, 35*(7), 29–32.
[13] Liu, A., Zhang, S., Wang, S., Wang, P., & Yan, G. (2022). Microscopic characteristics identification of ten medicinal materials with small fruits and seeds [In Chinese]. *Chinese Traditional Patent Medicine, 44*(6), 1869–1874.
[14] Yuan, S., Ma, Q., Chen, K., Liu, Y., Li, H., & Li, J. (2021). Micro-morphological identification of common mineral Chinese medicinal powders [In Chinese]. *Chinese Traditional and Herbal Drugs, 52*(5), 1454–1461.
[15] Buccino, F., Bagherifard, S., D'Amico, L., Zagra, L., Banfi, G., Tromba, G., & Vergani, L. M. (2022). Assessing the intimate mechanobiological link between human bone micro-scale trabecular architecture and micro-damages. *Engineering Fracture Mechanics, 270*, Article 108582.
[16] Liu, H., Han, D., Hu, J., Ren, L., & Tang, Y. (2024). Biomechanical functions analysis of the mallard webbed foot: A study of macroscopic and microscopic material assembly and tendon morphology. *Micron, 183*, Article 103648.
[17] Tu, Z., Xu, J., Dong, Z., Zhang, S., & Tan, J. (2025). Load-bearing optimization for customized exoskeleton design based on kinematic gait reconstruction. *Medical & Biological Engineering & Computing, 63*, 807–822.
[18] Ren, Z., Huang, J., Bai, H., Jin, R., Xu, F., & Xu, J. (2021). Potential application of entangled porous titanium alloy metal rubber in artificial lumbar disc prostheses. *Journal of Bionic Engineering, 18*, 584–599.